THE JOURNAL OF BIOLOGICAL CHEMISTRY
Vol. 277, No. 3, Issue of January 18, pp. 2225–2233, 2002
Printed in U.S.A.
© 2002 by The American Society for Biochemistry and Molecular Biology, Inc.

Inhibitory Module of Ets-1 Allosterically Regulates DNA Binding through a Dipole-facilitated Phosphate Contact*

Received for publication, October 1, 2001, and in revised form, October 31, 2001
Published, JBC Papers in Press, October 31, 2001, DOI 10.1074/jbc.M109430200

Hong Wang‡, Lawrence P. McIntosh§, and Barbara J. Graves‡¶

From the ‡Huntsman Cancer Institute, Department of Oncological Sciences, University of Utah, Salt Lake City, Utah, 84112-5550 and the §Department of Biochemistry and Molecular Biology and Department of Chemistry, University of British Columbia, Vancouver, British Columbia V6T 1Z3, Canada

DNA binding of the transcription factor Ets-1 is negatively regulated by three inhibitory helices that lie near the ETS domain. The current model suggests that this negative regulation, termed autoinhibition, is caused by the energetic expense of a DNA-induced structural transition that includes the unfolding of one inhibitory helix. This report investigates the role of helix H1 of the ETS domain in the autoinhibition mechanism. Previous structural studies modeled the inhibitory helices packing together and connecting with helix H1, suggesting a role of this helix in the configuration of an inhibitory module. Recently, high-resolution structures of the ETS domain-DNA interface indicate that the N terminus of helix H1 directly contacts DNA. The contact, which is augmented by the macrodipole of helix H1, consists of a hydrogen bond between the amide NH of leucine 337 in helix H1 and the oxygen of a corresponding phosphate. We propose that this hydrogen bond positions helix H1 to be a link between autoinhibition and DNA binding. Four independent approaches tested this hypothesis. First, the hydrogen bond was disrupted by removal of the phosphate in a missing phosphate analysis. Second, base pairs that surround the helix H1-contacting phosphate and appear to dictate DNA backbone conformation were mutated. Next, a hydrophobic residue in helix H1 that is expected to position the N terminus of the helix was altered. Finally, a residue on the surface of helix H1 that may contact the inhibitory elements was changed. In each case DNA binding and autoinhibition was affected. Taken together, the results demonstrate the role of the dipole-facilitated phosphate contact in DNA binding. Furthermore, the findings support a model in which helix H1 links the inhibitory elements to the ETS domain. We speculate that this helix, which is conserved in all Ets proteins, provides a common route to regulation.

In eukaryotes, conserved families of DNA-binding proteins regulate unique biological target genes despite binding to similar DNA sequences. The *ets* family of transcription factors is one such example in that all Ets proteins bind a core 5′-GGAA/T-3′ sequence through the conserved ETS domain (1, 2). The ETS domain displays a winged helix-turn-helix motif (Fig. 1), consisting of three α helices and four β strands (termed the wing). High-resolution crystal structures of four ETS domains (PU.1, GABPα, SAP-1, and Elk-1) in complex with DNA reveal that most of the conserved residues in the ETS domain make similar base-specific and phosphate contacts (3–7). Despite this common mode of DNA binding, each Ets protein is expected to regulate transcription of distinct genes. Multiple mechanisms lend specificity to ETS domain DNA binding (1, 2, 8). In the case of Ets-1, autoinhibition negatively regulates DNA binding and provides a route to specificity (reviewed in Ref. 9).

Autoinhibition is characterized by the observation that deletion or mutation of a region outside of a specific domain can modulate the activity of that domain. For example, in Ets-1, inhibitory elements that lie both N- and C-terminal to the ETS domain form a structural module that cooperatively represses the DNA binding activity of the ETS domain (10–13). Secondary structural studies by NMR spectroscopy demonstrate that the inhibitory module is composed of three helices: HI-1, HI-2, and H4 (Fig. 1, *A* and *B*) (14). Furthermore, the inhibitory module undergoes a conformational change upon binding to DNA. Our current model of autoinhibition hypothesizes that the energetic expense of this conformational change accounts for the relatively low DNA binding activity of the ETS domain in the presence of the inhibitory helices. The most dramatic feature of this conformational change is the unfolding of helix HI-1, which is detected by both protease sensitivity and circular dichroism (Fig. 1*B*) (13, 15). Although the unfolding of this helix is central to the autoinhibition mechanism, the existing experimental data do not provide a cause for this conformation change. For example, the inhibitory mechanism is not likely to work by steric interference because the inhibitory module, as modeled, does not directly occlude the contacts of the ETS domain with DNA.

Structural studies of the ETS domain-DNA interface and the inhibitory module provide molecular details that suggest helix H1 is the keystone of the autoinhibition mechanism. Comparing crystallographically determined models of the ETS domain-DNA complex (3–7), we observed that in addition to the helix-turn-helix motif the highly conserved helix H1 of the ETS domain also plays a role in DNA binding. Specifically, the amide NH of leucine 337 at the N terminus of helix H1 is within hydrogen bonding distance of an oxygen atom of a specific phosphate (Fig. 1*B*), yielding an interaction that is facilitated electrostatically by the macrodipole of helix H1 (16). This highly directional and distance dependent interaction is expected to be sensitive to the precise conformation of DNA and the orientation of the N terminus of helix H1 with respect to DNA. In addition, NMR studies of inhibited and activated forms of Ets-1 in the absence of DNA suggest that the inhibitory module packs against helix H1 (14, 17). Based on this

* This work was supported by grants from The National Institutes of Health (GM38663 to B. J. G. and CA24014 to the Huntsman Cancer Center) and the Huntsman Cancer Foundation. The costs of publication of this article were defrayed in part by the payment of page charges. This article must therefore be hereby marked "*advertisement*" in accordance with 18 U.S.C. Section 1734 solely to indicate this fact.

¶ To whom correspondence should be addressed: Huntsman Cancer Institute, University of Utah, 2000 Circle of Hope, Salt Lake City, UT 84112-5550. Tel.: 801-581-7308; Fax: 801-585-1980; E-mail: Barbara.Graves@hci.utah.edu.

This is an Open Access article under the CC BY license.

collection of structural information, we speculated that helix H1 could structurally and functionally couple the ETS domain to the inhibitory module (9). In our model, helix H1 in the unbound state contributes to the stability of the inhibitory module by direct interactions with both the inhibitory helices and the helix-turn-helix of the ETS domain. In the bound state, the N terminus of helix H1 directly contacts the phosphate backbone. We suggest that these two roles require alternative conformations of helix H1 with different packing interactions. Thus, DNA binding is accompanied by a change in helix H1 that destabilizes the inhibitory module. This potentially subtle change could involve an alteration in helix H1 structure and/or an adjustment in the orientation of the helix relative to other components.

To test this model we investigated the role of helix H1 in DNA binding and autoinhibition using two well characterized N-terminal deleted versions of murine Ets-1: ΔN280, which spans the intact inhibitory module as well as the ETS domain and displays full autoinhibition; and the further truncated ΔN331, which lacks the two N-terminal inhibitory helices and is fully de-repressed (Fig. 1*A*) (15). To probe the role of helix H1-DNA contact, we disrupted the hydrogen bond between helix H1 and phosphate oxygen directly by removing the phosphate or indirectly by changing the DNA sequence to alter its backbone conformation. In a complementary manner, we mutated amino acids in helix H1 that either pack against the helix-turn-helix of the ETS domain or connect the helix to the inhibitory module. Both classes of mutants affected autoinhibition. These findings support the hypothesis that the helix H1-phosphate contact contributes significantly to the ETS domain-DNA interaction. Furthermore, helix H1 connects to a network of intramolecular and intermolecular interactions that is essential for autoinhibition. This model suggests that helix H1 can serve as an allosteric control switch for both positive and negative regulation of ETS domain-DNA binding.

EXPERIMENTAL PROCEDURES

Site-directed Mutagenesis and Construction of Bacterial Expression Constructs—Mutagenesis was performed in high copy pET derivative (pAED) vectors containing murine Ets-1 cDNA that encoded ΔN280 or ΔN331 (15). Protein mutants L337I, L337V, L337A, Q339E were generated with PCR using the same C-terminal primer (5′-GCGGCTCAGCAGGATCCCTAGTCAGCATCCGGCTTTA-3′) and different N-terminal primers for each mutant. A *Bsp*120I site was introduced between nucleotides 999 and 1006 of the cDNA open reading frame of Ets-1 to facilitate this strategy. A *Bsp*120I-*Bam*HI fragment of the PCR product that encoded Ets-1 residues 333–440 with each mutation was subcloned into pAED-ΔN280 and pAED-ΔN331.

The N-terminal primer sequence for L337I, L337V, and L337A mutants is: 5′-GCGGGCCCATCCAG*XXX*TGGCAGCTTTC-3′, with the "*XXX* " positions as "ATC" for L337I, "GTG" for L337V, and "GCG" for L337A. The N-terminal primer sequence for Q339E mutant is: 5′-CGCGGGCCCATCCAGCTGTGGGAGTTTCTTCTGGAA-3′. Underlining denotes altered codon.

Protein mutants R409A, R409K, K404A were generated by QuickChange™ site-directed mutagenesis kit (Stratagene). The top strand primers for each mutant are as follows: 5′-GACGGCGGGCAAGGCCTACGTATACCGC-3′ (R409A), 5′-CCACAAGACGGCGGGCAAGAAGTACGTATACCGCTTTG-3′ (R409K), and 5′-GACAAAAATATCATCCACGCCACGGCGGGCAAGCGC-3′ (K404A).

Protein Expression and Purification—All versions of ΔN280 and ΔN331 were synthesized in *Escherichia coli* BL21λ (DE3);pLysS. Cultures of 500 ml were grown at 37 °C in L-broth, and protein expression was induced at midlog phase for 1.5 h by the addition of 1 mM isopropyl β-D-thiogalactopyranoside. Harvested cells were resuspended in 25 ml of lysis buffer (25 mM Tris-HCl, pH 7.9, 1 mM EDTA, 1 M KCl) with 1 mM phenylmethylsulfonyl fluoride and 10 mM dithiothreitol and lysed by sonication (Heat Systems, Inc.). All proteins were purified as described previously for wild type ΔN280 and ΔN331 (15). Purity was estimated to be greater than 90% by Coomassie Blue staining of SDS polyacrylamide gels. Protein concentrations were determined by spectrophotometry with calculated extinction coefficients (18) after denaturing in 6 M guanidine-HCl (Pierce).

Proteolysis Assays—Partial proteolysis assays on protein-DNA complexes were performed with trypsin in 20 μl of buffer (25 mM Tris, pH 8.5, 10 mM $CaCl_2$, 1 mM dithiothreitol) with 10 μM of ΔN280, each DNA duplex at 125 μM, and 0.05 μg of protease. The DNA duplex concentration was based on calculations that utilize affinity as well as total DNA and protein concentration to predict occupancy. We chose a DNA concentration that is predicted to give >99% protein in complex with all DNA duplexes tested. However, an experimental test with gel electrophoretic mobility shift assay (13) indicated that ~20% of the protein appeared to be unbound in two low-affinity nicked duplexes tested (nicked −2 and nicked +5′). We do not have an explanation for this phenomenon. Reaction mixtures were incubated at 25 °C for 0.5, 2, 5, and 10 min and were then stopped by adding SDS-PAGE sample buffer and incubated at 95 °C for 5 min. Digestion products were resolved on 18% SDS polyacrylamide gels and visualized by staining with Coomassie Blue. The intensities of the protein bands on the gel were quantified by Gel Doc 2000 (Bio-Rad).

Partial proteolysis assays on the ΔN280 mutants were performed as described above with 2 μg of wild type or mutant protein and 0.2 μg of protease. Reaction mixtures were incubated at 25 °C for 3 min and then stopped by adding SDS-PAGE sample buffer and incubated at 95 °C for 5 min. Digestion products were resolved on 18% SDS polyacrylamide gels and visualized by staining with Coomassie Blue.

Synthetic Oligonucleotides—Oligonucleotides were synthesized and subjected to trityl-affinity chromatography on an automated DNA synthesizer (Applied Biosystems 3948) followed by gel filtration on Biospin-6 (Bio-Rad). Both strands for unnicked DNA duplexes were 5′ end-labeled with T4 polynucleotide kinase and [γ-^{32}P]ATP (4500 Ci/mol) and annealed as described previously (13). For nicked DNA duplexes, the intact strand and one of the two complementary strands were labeled such that the nick would have two free hydroxyls. After labeling reactions were stopped, the second complementary strand was added, and these strands were annealed to generate nicked DNA duplexes.

The 9-bp high-affinity binding site, termed SC1 (11), was used as the Ets-1 recognition site in all assays. A 27-bp duplex (SC1–27) was used in DNA binding assays with protein mutants and served as the parental duplex for mutated DNA duplexes. Nicked duplexes that are missing right flank phosphates were based on SC1–27. A 35-bp duplex (SC1–35) was used as the parental duplex for nicked duplexes that are missing left flank phosphates. The sequences for the parental duplexes were: 5′-GCCAAGCCGGAAGTGTGTGGTAAGCAG-3′ (top strand, SC1–27), 5′-CTGCTTACCACACACTTCCGGCTTGGC-3′ (bottom strand, SC1–27), 5′-GAATATGGGCCAAGCCGGAAGTGTGTGGTAAGCAG-3′ (top strand, SC1–35), and 5′-CTGCTTACCACACACTTCCGGCTTGGCCCATATTC-3′ (bottom strand, SC1–35).

DNA Binding Assays—Equilibrium dissociation constants (K_D) were measured by quantitative electrophoretic mobility shift assay. In brief, binding reactions in a 20-μl volume containing of 25 mM Tris-HCl (pH 7.9), 10% glycerol, 1 mM EDTA, 50 mM KCl, 6 mM $MgCl_2$, 0.1 mg/ml bovine serum albumin, and 1 mM dithiothreitol were incubated for 20 min at 4 °C to reach equilibrium. Protein concentration was varied, whereas the DNA concentrations were kept constant and below 10^{-11} M. Electrophoresis was performed at 4 °C on 6% native polyacrylamide gels as described previously (13). Gels were run at 30 V/cm for 1.5 h and dried on filter paper. Radioactivity was quantified by PhosphorImager (Molecular Dynamics). Equilibrium dissociation constants (K_D) were determined by plotting the fraction of bound DNA ([DP]/[Dt]) *versus* the concentration of free protein ([P]) (13). K_D values were obtained by nonlinear least square fitting of the mean data points to the rearranged equilibrium equation $[PD]/[Dt] = 1/(1+(K_D/[P]))$ (KaleidaGraph, version 3.0, Synergy Software). The total concentration of DNA ([Dt]) was kept at least 20-fold below the expected K_D of the Ets-1 species, allowing the assumption that [P] is equal to the total protein concentration ([Pt]) in the binding reaction. Data points are the mean values from two experiments. Error bars represent the standard deviation of the mean for each point.

RESULTS

Deletion of the Phosphate That Contacts Helix H1 Affected DNA Binding and Autoinhibition—To evaluate the role of the helix H1-phosphate contact, we undertook a biochemical approach to the study of the importance of all phosphate contacts within the ETS domain-DNA interface. Phosphate contacts were defined previously by structural analyses as well as biochemical studies, such as ethylation interference and hydroxyl

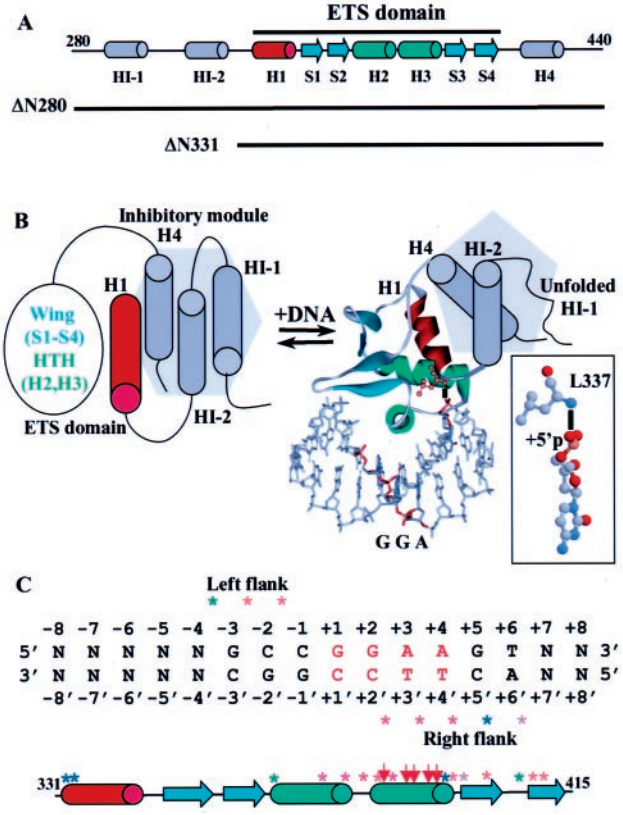

FIG. 1. **Summary of ETS domain-DNA interaction and model of autoinhibition.** *A*, schematic representation of the secondary structure of ETS domain and inhibitory elements as determined by NMR spectroscopy (14, 17, 46). Indicated Ets-1 species, ΔN280 and ΔN331, include residues 280–440 and 331–440, respectively. *B*, model of Ets-1 autoinhibition. The *shaded areas* on both panels represent the modeled structure of inhibitory module. The secondary helical structures are firmly established, whereas the helical packing and interaction with the ETS domain are modeled from changes in NMR chemical shifts (14). The shape of the *shaded area* changes upon binding to DNA, reflecting a conformation change that includes the unfolding of helix HI-1 as determined by circular dichroism and partial proteolysis (15). The ETS domain in complex with DNA (*right panel*) is based on crystal structure coordinates of the GABPα ETS domain bound to DNA (4). GABPα and Ets-1 display strong conservation within the ETS domain (2). The GGA represents the invariant recognition sequence. The dipole-driven hydrogen bond between the amide NH of Leu-337 and +5′p oxygen is *highlighted*. *C*, summary of the protein-DNA interactions shared by Ets proteins. *Top panel*, The 9-bp SC1 binding site (11) containing the invariant GGA sequence is presented with flanking base pairs (Ns) that are necessary for sequence specific high affinity interaction but show no sequence preference (47). A numbering system is provided, with the phosphates designated as the 5′ phosphate of a nucleotide. Contacted bases are shown in *red*, and the *colored asterisks* indicate the contacted phosphates. *Bottom panel*, positions of protein residues that are making DNA contacts as determined by crystallographic studies. *Red arrows* indicate residues that are making base-specific contacts. *Asterisks* mark the residues making phosphate contacts and are color-coordinated with the *top panel*.

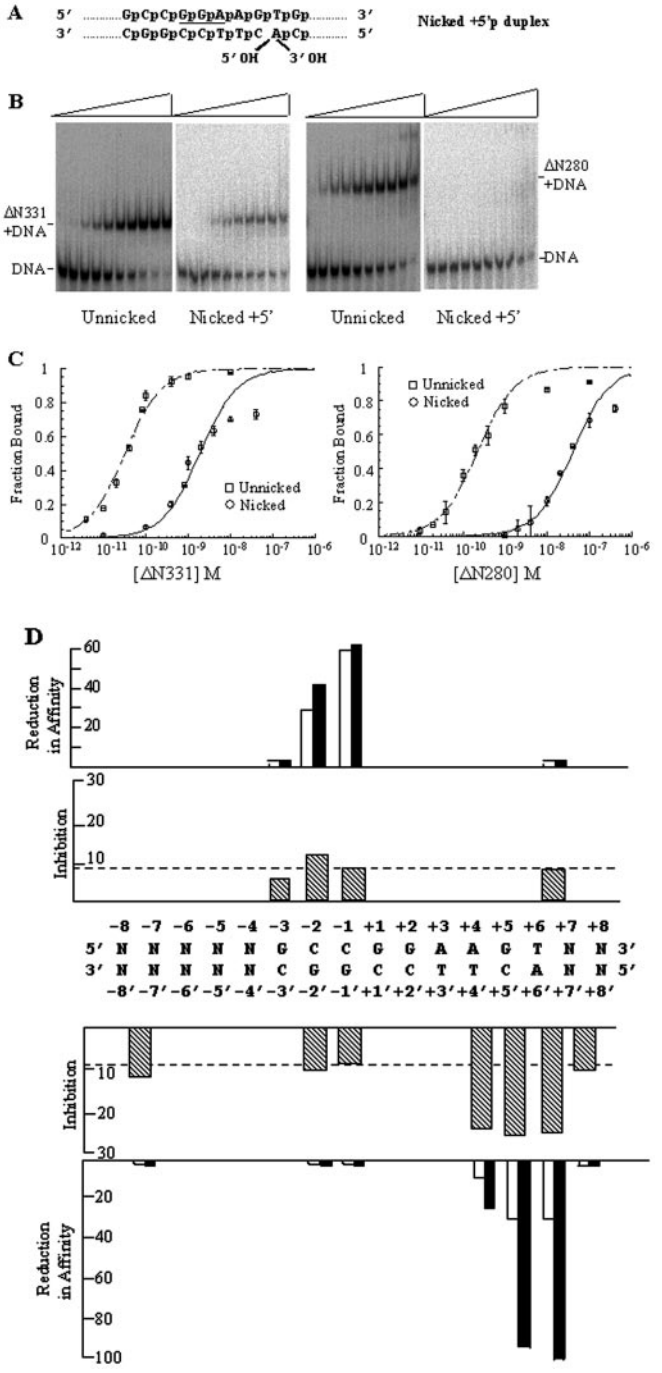

FIG. 2. **Missing phosphate assay identifies phosphate contacts important for DNA binding and autoinhibition.** *A*, a scheme of the SC1 site duplex nicked at +5′p. *B*, phosphorimage of electrophoretic mobility shift assay of ΔN331 (*left two panels*) and ΔN280 (*right two panels*) for SC1 duplex unnicked and nicked at +5′p. The *wedge* indicates increasing amounts of corresponding Ets-1 species in each binding reaction (10^{-12}-10^{-6} M). *C*, equilibrium DNA binding curves for ΔN331 and ΔN280 (data from *B* and two replicas). *D*, summary of "missing phosphate" experiment data. *Open* and *closed bars* display the reduction in affinity of ΔN331 and ΔN280, respectively, for nicked duplexes relative to unnicked duplex: K_D(nicked)/K_D(unnicked). *Shaded bars* represent the level of inhibition for nicked duplexes: K_D(ΔN280)/K_D(ΔN331). The *dotted lines* represent the level of inhibition (8-fold) for unnicked duplex. See Table I for K_D and error values.

radical protection assays (11, 19–21). These approaches implicated the phosphate contacted by helix H1 (+5′p; see Fig. 1*C* legend for the numbering of phosphates) as well as five other phosphates (left flank −2, −1; right flank +2′, +3′, +4′). We measured the energetic contribution of five of these phosphates, as well as six other sites, by using nicked DNA duplexes that removed individual phosphates (Fig. 2*A*). In this "missing phosphate" assay (22) DNA binding affinities, expressed as equilibrium dissociation constants (K_D), were determined by quantitative electrophoretic mobility shift assays (Fig. 2, *B* and *C*). The loss of a phosphate at positions that are not predicted to contact the protein (−8′, −2′, −1′, and +6) displayed no reduction in affinity for either ΔN331 or ΔN280 (Fig. 2*D*, Table I). These controls are consistent with structural data indicating that a gap in the phosphodiester backbone causes a local rather than a global conformation change of a DNA duplex (23–28).

TABLE I
DNA binding affinities from "missing phosphate assay" indicate that right flank phosphates play a role in autoinhibition

Nicked position	ΔN331		ΔN280		Inhibition[c]
	K_D[a]	Reduction in affinity[b]	K_D[a]	Reduction in affinity[b]	
	0.1 nM	*-fold*	*0.1 nM*	*-fold*	
SC1–27[d]	0.30 ± 0.03	1	2.4 ± 0.2	1	8 ± 1
+6	0.40 ± 0.03	1.3	3.2 ± 0.3	1.3	8 ± 1
+6′	0.40 ± 0.04	1.3	4.8 ± 0.5	2.0	12 ± 2
+5′	9.3 ± 0.7	31	240 ± 24	100	26 ± 3
+4′	8.2 ± 0.9	27	214 ± 20	89	26 ± 4
+3′	2.3 ± 0.2	7.7	57 ± 6	24	25 ± 3
SC1–35[d]	0.41 ± 0.04	1	3.3 ± 0.3	1	8 ± 1
−3	0.92 ± 0.1	2.2	5.0 ± 0.4	1.5	5.4 ± 0.7
−2	11 ± 1	27	129 ± 10	39	12 ± 1
−1	22 ± 3	54	191 ± 18	58	9 ± 1
−3′	0.38 ± 0.04	0.9	4.3 ± 0.4	1.3	11 ± 2
−2′	0.45 ± 0.06	1.1	4.3 ± 0.5	1.3	10 ± 2
−8′	0.45 ± 0.05	1.1	5.6 ± 0.6	1.7	12 ± 2

[a] K_D was derived from binding isotherm as in Fig. 2. Values are means (±S.D.) of two to three independent experiments.
[b] Reduction in affinity was determined by dividing the K_D for each nicked duplex by that of the parental unnicked duplex.
[c] Inhibition is K_DΔN280/K_DΔN331. Errors are calculated based on the propagation of errors from K_DΔN331 and K_DΔN280.
[d] Two different parental unnicked duplexes were used in these experiments. See "Experimental Procedures" for details.

To evaluate the importance of phosphates within the DNA-protein interface, we measured the binding activity of ΔN331 on nicked duplexes (Fig. 2*D*, Table I). Positions −3 and +6′ showed modest sensitivity to phosphate loss with only a 1.3-fold reduction in affinity. These are positions at which Ets-1 contacts DNA; however, these contacts are observed in only a subset of ETS domain-DNA structures. In contrast, positions −2, −1, +3′, +4′, and +5′), at which phosphates are contacted in all known ETS domain-DNA structures and that show ethylation interference, displayed a larger reduction of affinity (7.7–54-fold). The range of affinities represents a change in free energy (ΔΔG°) of 1.1- 2.2 kcal/mol and is within the range expected for the loss of one to several electrostatic interactions. These results demonstrate that phosphate contacts play a significant role in DNA binding of the ETS domain and that contacts conserved among all Ets proteins are relatively more important.

To investigate the role of phosphate contacts in the autoinhibition mechanism, we compared the DNA binding affinity of ΔN280 to that of ΔN331 on each nicked duplex. In previous studies performed on an unnicked duplex, ΔN280 and ΔN331 display a 10-fold difference in affinity (15). As expected, a similar level of inhibition (8 to 12-fold) was observed with duplexes nicked at sites not contacting protein (+6, −8′, −2′, −1′, +6′; Fig. 2*D*, Table I). Duplexes nicked at sites that form key contacts on the left flank (−1 and −2) caused a similar reduction in affinity of both ΔN280 and ΔN331 and thus retained nearly normal levels of autoinhibition (9- and 12-fold; Fig. 2*D*, Table I). In contrast, the loss of the right flank phosphates (+3′, +4′, and +5′) caused a larger reduction of affinity for ΔN280 than for ΔN331. For example, the loss of +5′ phosphate reduced DNA binding affinity ~100-fold for ΔN280 compared with only 31-fold for ΔN331. This result suggested that removal of this right flank phosphate contact leads to a 3-fold increase in the level of autoinhibition. We will discuss this result after additional data are presented.

We were surprised that removal of phosphates +3′ and +4′ affected autoinhibition to the same degree as removal of the helix H1-contacting +5′ phosphate. However, a more careful analysis of the ETS domain-DNA interface of the highly related GABPα, which has been described by crystallography, suggested that these phosphates are within a network of intermolecular and intramolecular interactions involving the helix H1-+5′ phosphate contact (4). Thus, removal of any phosphate contact within this network could affect the helix H1-DNA interaction. In contrast, removal of a phosphate contact that is distant from this network (*e.g.* left flank phosphates −3, −2, −1) reduced DNA binding to various degrees but minimally affected the level of autoinhibition.

Altered DNA Backbone Conformation Affected DNA Binding and Autoinhibition—To further investigate the importance of the helix H1-phosphate contact, we focused our attention on the nucleotide sequences around +5′p. We observed a 5′ purine-pyrimidine (RY) 3′ preference around the +5′ phosphate in binding site selection experiments for several Ets proteins. This preference, which recapitulates that found in many promoter sequences (Table II and references therein), exists despite the lack of hydrogen bonding to base pairs in this part of the DNA-protein interface (3–5, 7). We suggest that protein binding to this region recognizes the sequence-dependent conformation of the DNA backbone. This phenomenon of indirect read-out has been reported in a variety of DNA-protein complexes including MetJ, *Eco*RI, *Eco*RV, SAP-1, and a variety of helix-turn-helix proteins (5, 29–32). Considering the requirement for proper distance and direction to form the hydrogen bond between the amide NH of leucine 337 and +5′p, we predicted that the DNA conformation around this phosphate would be important to precisely present the oxygen of this phosphate to the amide NH.

To test this hypothesis, base substitutions were introduced into nucleotide positions 5 and 6 in the DNA binding site, and the effects on DNA binding of ΔN331 were measured (Table III and Fig. 3). Single purine or pyrimidine transitions (from GT to AT or GC) showed no change in binding affinity. Single transversion at either one of the two positions (GT to CT, GA, or GG) reduced the binding affinity 2.5 to 4-fold. Double transversions (GT to CA or TG) reduced the binding affinity 5- and 16-fold, respectively. These results are consistent with the RY sequence preference dictating the DNA backbone conformation that in turn precisely positions the phosphate oxygen for hydrogen bonding with the amide NH of leucine 337.

Next, to investigate the importance of +5′ phosphate positioning for the autoinhibition mechanism, these variant duplexes were tested for binding to ΔN280. A single transition or transversion only modestly reduced DNA binding (1.4-, 4-, and 6-fold, respectively) in ΔN280 and had no effect on the level of autoinhibition (8- and 13-fold, respectively). However, the double transversions caused a 3–5-fold increase in autoinhibition. This effect was similar to that caused by the removal of right flank phosphates in the missing phosphate assay. We suggest

TABLE II
Conservation of purine-pyrimidine around +5′ phosphate in selected consensus of binding sites for ets proteins

Proteins[a]	Selected consensus[b] RY[c]	References
Ets-1	ACCGGAAGT g a TaC	(11)
GABPα	GCCGGAAGT aga tac	(48)
PU.1	AAAAAGAGGAAGTAG tcC c GC	(49)
Elk-1	AACCGGAAGTG A	(50)
SAP-1	ACCGGAAGT tac	(50)

[a] The Ets proteins with high-resolution structures plus Ets-1. For additional comparisons, see Ref. 2.
[b] Consensus sequences were selected using DNA duplexes with either randomized sequences or fixed GA (GABPα), GGA (Ets-1) in the middle of the sequences. Nucleotides in lowercase letters were less frequently selected.
[c] Positions of nucleotides that display preference for purine (R) and pyrimidine (Y), respectively.

that the reversal of the preferred RY motif sufficiently changed the DNA backbone conformation to affect the +5′ phosphate-helix H1 contact. Importantly, mutations of other regions of the binding site that also reduce DNA binding affinity have no effect on the level of autoinhibition (33).

Removal of +5′ Phosphate Affected Conformational Change of the Inhibitory Module—In both of the DNA analyses above, the loss of the helix H1-phosphate interaction caused a more severe reduction in the binding of ΔN280 than ΔN331 and thus an apparent enhancement of autoinhibition. One possible explanation is that the DNA-induced conformational change in the inhibitory module is not efficiently induced upon binding to altered DNA duplexes. This would lead to retention of a structured inhibitory module in the bound protein and result in reduced affinity.

To test this hypothesis we investigated the structural status of the inhibitory helix HI-1 in binding complexes with unnicked and nicked duplexes by partial proteolysis (Fig. 4). Previous studies established that the conformation change accompanying DNA binding generates a 16-kDa tryptic fragment due to cleavage immediately C-terminal to helix HI-1. The enhanced sensitivity of this site in the presence of DNA corresponds to the unfolding of helix HI-1 (15). As expected, generation of the 16-kDa fragment was enhanced in the presence of unnicked DNA duplex (3.4-fold increase in proteolysis efficiency at 10 min; Fig. 4). In contrast, a duplex nicked at +5′p caused only 1.8-fold increase, indicative of a more structured inhibitory module. A control experiment with a duplex nicked at +6p confirmed that this reduction (from 3.4 to 1.8-fold) was not due to the presence of a nick. However, a control duplex nicked at −2p, which displays the same relatively low affinity ($K_D \sim 10^{-8}$ M) but a normal level of autoinhibition (Table I; Fig. 2*D*), showed only a 2.6-fold increase in proteolysis efficiency. This suggested that the protease susceptibility measured for the nicked +5′p duplex was due in part to its low affinity. We noted in an electrophoretic mobility shift assay that only ~80% of ΔN280 was in complex with the low affinity −2p and +5′p nicked duplexes even with the large excess of DNA (data not shown). The presence of unbound protein would contribute to a reduced level of proteolysis. Despite this limitation of the assay system, these results suggest that binding with nicked +5′p duplex reduced the protease susceptibility of helix HI-1 more than the nicked −2p control. We conclude that DNA binding to nicked +5′p duplex was less efficient in causing the conformational change in the inhibitory module than an intact duplex. These findings indicated that the helix H1-phosphate contact is critical for the DNA-induced conformational change.

In summary, both the missing phosphate assay and DNA mutational analysis altered the helix H1-phosphate contact and reduced affinities for both ΔN331 and ΔN280. Furthermore, the effects were more severe on ΔN280, resulting in an apparent enhancement in autoinhibition. Partial proteolysis studies indicated that the inhibitory module appears to be more structured in ΔN280 bound to nicked +5′p duplex. We propose that retention of some structure causes a severe reduction in affinity and the apparent enhancement of inhibition. The results of these DNA alteration experiments indicated that helix H1 is an important part of a network of intermolecular and intramolecular interactions that provides a connection between DNA binding and autoinhibition. In the next set of experiments, mutagenesis of the protein is used to identify other parts of this network.

Altered Position of the N Terminus of helix H1 Uncoupled the Inhibitory Module from ETS Domain DNA Binding—Our model for the role of helix H1 in autoinhibition predicts that mutation of residues in this helix would affect autoinhibition, whereas those within other structural elements would have no effect. We designed three classes of mutant proteins to test this prediction (Fig. 5). The first class of mutants tested the hypothesis that the phosphate contact made by the peptide backbone amide of helix H1 plays a key role in DNA binding and autoinhibition. The goal was to alter the precise orientation of the N terminus of helix H1 by disruption of the hydrophobic contacts between the helix and the core of ETS domain. We predicted that such a disruption would disconnect DNA binding from the inhibitory mechanism. Based on structural data showing that leucine 337, located at the N terminus of helix H1, interacts with the hydrophobic core of the ETS domain (Figs. 1*B* and 5, *A* and *B*), we reasoned that mutations in the side chain of this residue would perturb the helix H1 packing to other parts of the ETS domain.

The ΔN331 mutations L337I, L337V, and L337A caused a graded reduction of DNA binding affinity (22 to 200-fold) as the hydrophobic side chain is progressively changed in the order of isoleucine, valine, and alanine (Table IV, Class I). These results suggest that the disruption of the hydrophobic packing of helix H1 alters the structure, perhaps simply by increasing the flexibility of the N terminus, such that the amide NH is not precisely positioned to form the optimal hydrogen bond with +5′p. The large effect on DNA binding for $\Delta N331^{L337V}$ (170-fold) and $\Delta N331^{L337A}$ (200-fold), which represent $\Delta\Delta G^o$ of 2.8 and 2.9 kcal/mol, respectively, may not be due to the loss of only one hydrogen bond. Potentially, the loss of one critical hydrogen bond and/or the hydrophobic packing involving leucine 337 affects a network of intermolecular and intramolecular interactions within the DNA-protein complex. For example, it could indirectly affect the helix-turn-helix (H2 and H3), thereby altering contacts to bases in the major groove.

Dramatically, Class I mutants displayed almost the same affinity within the ΔN280 and ΔN331 contexts (Table IV). Thus, autoinhibition was partially or completely abrogated. This finding suggests that the inhibitory module in these mutants has lost the ability to regulate DNA binding of Ets-1. We speculate that this loss of autoinhibition is due to the increased flexibility of the N terminus of helix H1 relative to other structural elements in these mutants. We propose that the lack of a rigid structural connection between helix H1 and the hydrophobic core of ETS domain severely weakens the functional link between DNA binding and the folded inhibitory module. These findings suggest that the interactions between helix H1 and the rest of the ETS domain are important parts of the

TABLE III
DNA binding affinities for mutant duplexes indicate that indirect read-out at right flank phosphate +5′ plays a role in autoinhibition

DNA	ΔN331		ΔN280		Inhibition[c]
	K_D[a]	Reduction in affinity[b]	K_D[a]	Reduction in affinity[b]	
	0.1 nM	*-fold*	*0.1 nM*	*-fold*	
RY (GT)	0.30 ± 0.03	1	2.4 ± 0.2	1	8 ± 1
RY (GC, AT)	0.42 ± 0.05	1.4	3.4 ± 0.5	1.4	8.1 ± 1.5
RR (GA, GG)	0.75 ± 0.07	2.5	9.6 ± 2	4.0	13 ± 3
YY (CT)	1.2 ± 0.2	4.0	15 ± 3	6.0	13 ± 3
YR (CA)	1.5 ± 0.2	5.0	60 ± 10	25	40 ± 9
YR (TG)	4.8 ± 0.8	16	130 ± 8	55	27 ± 5

[a] K_D was derived from binding isotherm as in Fig. 2. Values are means (±S.D.) of two to three independent experiments.
[b] Reduction in affinity was determined by dividing the K_D for the indicated duplex by that of the wild type RY (GT) duplex.
[c] Inhibition is K_DΔN280/K_DΔN331. Errors are calculated based on the propagation of errors from K_DΔN331 and K_DΔN280.

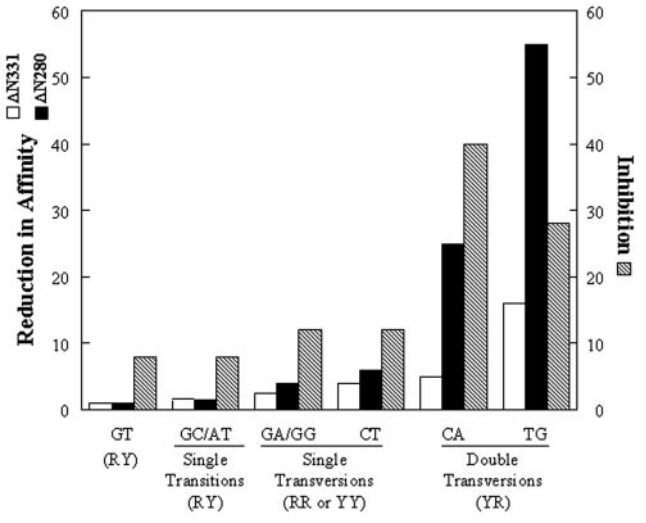

FIG. 3. **Mutagenesis of right flank nucleotides demonstrates indirect read-out and its role in autoinhibition.** *Open* and *closed bars* represent the relative affinity of ΔN331 and ΔN280, respectively, for mutant duplex relative to parental duplex: K_D(mutant)/K_D(parental). *Shaded bars* represent the fold of inhibition: K_D(ΔN280)/K_D(ΔN331). See Table III for K_D and error values.

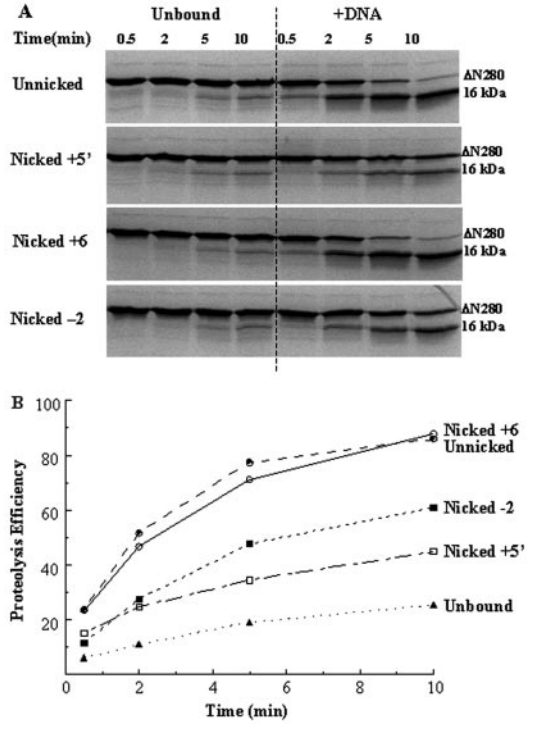

FIG. 4. **Partial proteolysis analyses of ΔN280 in complex with DNA duplexes detect changes in inhibitory module conformation.** *A*, SDS-PAGE images of partial trypsin proteolysis of preformed protein-DNA complexes with either unnicked or nicked DNA duplexes. *B*, proteolysis efficiency for each DNA duplex plotted against time. Proteolysis efficiency was defined by the intensity of the 16-kDa band divided by the total intensity of the 16-kDa band and the ΔN280 band at each time point. The proteolysis efficiency at 10 min was used to obtain the fold enhancement of proteolysis efficiency reported in the text for each DNA duplex. Experiments have been repeated at least once, and the same relative effects on proteolysis efficiency were observed for each DNA duplex.

network that mediates autoinhibition.

In the second class of mutants, which served as controls for Class I mutants, we changed residues that contact DNA but are distant from helix H1. These "wing" mutations (K404A, R409A, and R409K; Fig. 5) were expected to reduce DNA binding affinity but not to affect the position of the N terminus of helix H1. As predicted, the phenotypes of this class of mutants displayed moderate to severe reduction on DNA binding affinity in the ΔN331 context (6-fold for R409A, 460-fold for K404A; Table IV). Side chains emanating from the wing interact only with phosphates. Thus, these data confirmed the importance of DNA backbone interactions as detected in previous analyses. Autoinhibition was observed close to the normal level with the exception of K404A mutants. The apparent 3-fold enhancement of autoinhibition may be due to the low affinity of the ΔN280 version of this mutant ($K_D = 10^{-7}$ M), which is in the range of less accurately measured nonspecific binding. The results from this class of mutants demonstrated that autoinhibition in the 8–12-fold range is retained in proteins with a wide range of DNA binding affinity. In addition, mutations that are unlikely to affect helix H1 structure or its alignment do not significantly impact the level of inhibition.

To control for the potential effects of mutagenesis on overall protein folding and stability, ΔN280 Class I and Class II mutants were subjected to partial trypsin proteolysis (Fig. 6, *A* and *B*). Four of these mutants displayed a resistance to cleavage that was similar to wild type ΔN280, indicating no effect on the overall protein structure. $\Delta N280^{L337A}$ was more easily degraded, suggesting that some protein molecules were not folded properly and that the measurements for this mutant might underestimate the affinity.

Disruption of the Helix H1-Inhibitory Module Interface Relieved Autoinhibition—In the third class of mutants we investigated the structural connection between helix H1 and the inhibitory helices. According to our model, disruption of the inhibitory helix packing or the connection between helix H1 and the inhibitory helices could relieve inhibition. Indeed, mutation of leucine 429 to alanine, which alters a residue on the surface of helix H4 (Fig. 5*A*), results in the predicted enhanced DNA binding affinity in the context of both the full-length Ets-1 and ΔN280 (34–36). Ets-1^{L429A} and $\Delta N280^{L429A}$ display constitutive unfolding of inhibitory helix HI-1 as shown by the en-

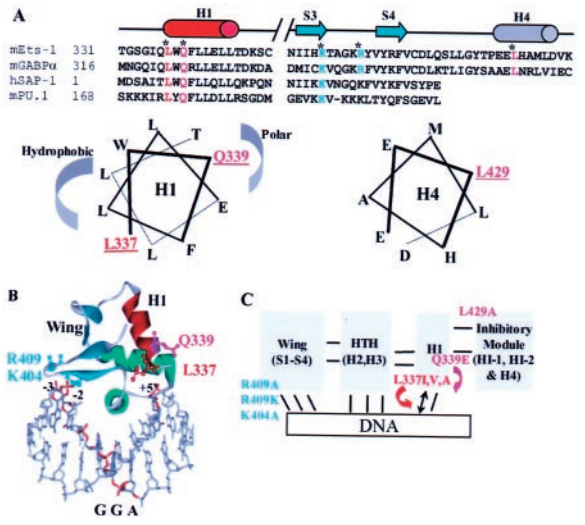

FIG. 5. **Protein mutations that affect DNA binding affinity and autoinhibition demonstrate the role of helix H1.** *A*, sequence alignment of helix H1, S3, S4, and H4 residues of four Ets proteins. Each mutated residue is indicated by an *asterisk*, with Class I mutants *highlighted* in *red*, Class II mutants in *cyan*, and Class III mutants in *purple*. *B*, crystal structure of ETS domain-DNA complex (4) (see Fig. 1 legend for comments) with the mutated residues and the contacting phosphates *highlighted*. *C*, schematic representation of the protein-DNA interaction network. The *solid lines* between each structural unit represent interactions. The *double-headed arrow* between helix H1 and DNA represents the dipole-driven phosphate contact. The *curved arrows* indicate the indirect effects of Q339E and Leu-337 mutants on DNA binding.

hanced protease cleavage near HI-1 to generate the 16-kDa tryptic fragment (Figs. 1*B* and 6*C*) (13, 34). This conformational change was previously thought to be an inherent part of the autoinhibition mechanism due to the correlation between the constitutively unfolded helix HI-1 and enhanced binding activity. On the other hand $\Delta N331^{L429A}$, which is missing inhibitory helices HI-1 and HI-2, had normal levels of DNA binding (Table IV, Class III). These data indicate that leucine 429 plays no role in DNA binding but rather assists in the intramolecular packing of the inhibitory module and/or connects the module to helix H1 (Fig. 5*C*). Higher resolution structural data are necessary to understand the exact role of leucine 429 in inhibitory module packing.

Our model predicts that residues on helix H1 also play a role in the packing of the inhibitory module. Strong candidates for this interaction would be residues on the surface of helix H1 that faces away from the hydrophobic core of ETS domain. According to high-resolution structural data, glutamine 339 is on this surface (Fig. 5, *A* and *B*). Unexpectedly, mutation of glutamine 339 to glutamic acid reduced DNA binding 16-fold in the context of ΔN331 (Table IV, Class III). In the crystallographically derived structure of the GABPα/β-DNA complex, the side chain of glutamine 324 (corresponding to glutamine 339 in Ets-1) interacts with glutamine 321 (corresponding to glutamine 336 in Ets-1), which in turn makes direct phosphate contact (4). This linkage potentially explains the reduction of DNA binding for $\Delta N331^{Q339E}$ (Fig. 5*C*). More relevant to our prediction, the affinity of $\Delta N280^{Q339E}$ and $\Delta N331^{Q339E}$ differed by only 3.5-fold (Table IV, Class III), representing a 2.3-fold reduction of autoinhibition. Furthermore, $\Delta N280^{Q339E}$ displays enhanced protease sensitivity at the cleavage site near helix HI-1 (Fig. 6*C*) indicating that the inhibitory module in this mutant is disrupted in a manner similar to $\Delta N280^{L429A}$. This result is consistent with the reduced level of inhibition for this mutation. Taken together, the mutagenesis study on glutamine 339 indicates that this residue plays a role in connecting the inhibitory module to helix H1 of the ETS domain. Furthermore, this and other possible connections between helix H1 and the inhibitory module are essential parts of the network of interactions that allosterically regulates DNA binding of Ets-1.

DISCUSSION

Helix H1 Links Inhibitory Module to DNA Binding—Previous studies of autoinhibition in Ets-1 discovered an order-to-disorder conformational change in the inhibitory module upon binding to DNA. This report identifies a network of interactions centered on helix H1 that could mediate this structural transition (Fig. 5*C*). We speculate that DNA binding by helix H1 changes this network, thereby allosterically inducing the conformational change in the inhibitory module. Three lines of evidence support this proposal. First, disruption of the hydrogen bond between +5′ phosphate and leucine 337 by removal of the phosphate or by a change in DNA conformation enhanced the apparent level of autoinhibition. This was due in part to the partial uncoupling of DNA binding and the conformational change of the inhibitory module, as evidenced by partial proteolysis. Second, disruption of this phosphate contact by affecting the precise position of the N terminus of helix H1 (Class I protein mutants) lowered DNA binding affinity and significantly reduced autoinhibition. Third, disruption of the connection between the inhibitory module and helix H1 (Class III protein mutants) resulted in partial or complete loss of autoinhibition. As important controls, disruption of phosphates in other parts of the binding site or mutation of residues that are not structurally connected to the inhibitory module (Class II mutants) strongly reduced DNA binding affinity but retained autoinhibition.

Interestingly, alterations of the DNA binding site retained and even enhanced the difference in affinity between ΔN280 and ΔN331, whereas protein mutations in helix H1 almost completely eliminated the differential between these two species. In the two DNA analyses reported here, the alterations caused the +5′ phosphate to be missing or in a suboptimal position. We suggest that these changes result in a loss or weakening of hydrogen bonding between leucine 337 and DNA and thus lowered affinity of both ΔN331 and ΔN280. In ΔN280, the DNA alteration weakens the connection between DNA binding and the inhibitory module and results in a more structured inhibitory module, as reflected in its protease sensitivity. We suggest that the structured inhibitory module severely compromises DNA binding by affecting parts of the DNA-protein interface in addition to the +5′ phosphate contact. In contrast, mutation of protein elements altered the packing between helix H1 and the helix-turn-helix core (Class I mutants) or between helix H1 and the inhibitory module (Class III mutants). These alterations likely disrupt intramolecular interactions and provide more flexibility for positioning the N terminus of helix H1. Thus, the inhibitory module in these mutants is structurally or dynamically uncoupled from the ETS domain, leading to a partial or complete loss of the ability to regulate DNA binding.

These findings provide a structural and mechanistic model of Ets-1 autoinhibition that focuses on a molecular network surrounding helix H1 (Figs. 5*C* and 7). Helix H1 participates in a hydrogen bond (between amide NH of Leu-337 and +5′p) that is augmented by the macrodipole of helix H1 and is highly dependent on the conformation of both the DNA and protein. The DNA backbone conformation is tightly controlled by the purine-pyrimidine sequence preference in the region. The precise presentation of the amide NH of Leu-337 is established by the position of the N terminus of helix H1. This conformation of helix H1 is regulated by a network of interactions, including the electrostatic contacts to DNA involving the macrodipole of

TABLE IV
DNA binding affinities for protein mutants indicate helix H1 is linked to both the helix-turn-helix and inhibitory elements

Class	Mutant	Region	ΔN331		ΔN280		Inhibition[c]
			K_D[a]	Reduction in affinity[b]	K_D[a]	Reduction in affinity[b]	
			0.1 nM	*-fold*	*0.1 nM*	*-fold*	
WT			0.30 ± 0.03	1	2.4 ± 0.2	1	8 ± 1
I	L337I	H1	6.6 ± 0.4	22	20 ± 5	8.3	3.0 ± 0.8
	L337V	H1	51 ± 5	170	120 ± 32	50	2.4 ± 0.7
	L337A[d]	H1	60 ± 6	200	101 ± 16	42	1.7 ± 0.3
II	R409A	Wing	1.9 ± 0.1	6.3	36 ± 8	15	19 ± 4
	R409K	Wing	3.3 ± 0.7	11	23 ± 3	9.6	7 ± 2
	K404A	Wing	140 ± 16	470	4000 ± 400	1700	28 ± 4
III	Q339E	H1	4.9 ± 0.8	16	17 ± 2	7.1	3.5 ± 0.7
	L429A[e]	H4	0.37 ± 0.05	1.2	0.51 ± 0.04	0.21	1.4 ± 0.2

[a] K_D was derived from binding isotherm as in Fig. 2. Values are means (±S.D.) of two to three independent experiments.
[b] Reduction in affinity was determined by dividing the K_D for each mutant by that of the wild type (WT) protein.
[c] Inhibition is K_DΔN280/K_DΔN331. Errors are calculated based onthe propagation of errors from K_DΔN331 and K_DΔN280.
[d] This mutant has been described previously in both the ΔN331 and ΔN280 forms (47).
[e] This mutant has been described previously in the ΔN280 form (35).

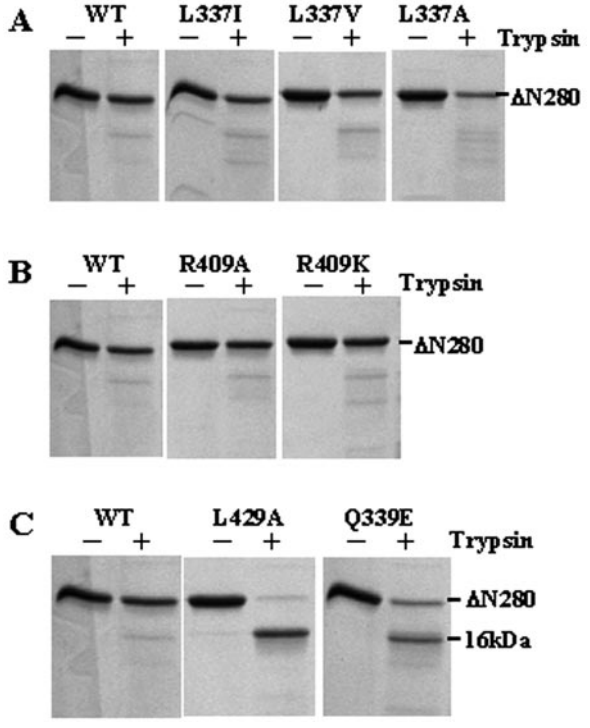

FIG. 6. **Partial trypsin proteolysis analyses of mutant ΔN280 proteins.** Wild type (*WT*) or mutant ΔN280 (2 μg) was mixed with 0.2 μg of trypsin (+) or mock-treated (−). *A*, Class I mutants; *B*, Class II mutants; *C*, Class III mutant.

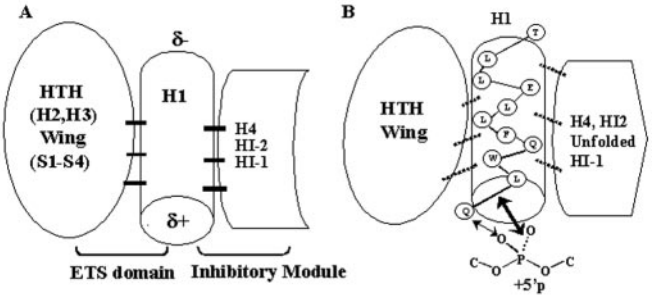

FIG. 7. **Model of helix H1 as a regulatory point for autoinhibition mechanism.** *A*, schematic representation of the unbound state of the ETS domain and inhibitory module. The *lines* between each structural module represent intramolecular interactions. The direction of the macrodipole of helix H1 is indicated by δ− and δ+. *B*, schematic representation of the bound state of the ETS domain and inhibitory module. The *arrows* between helix H1 and +5′p represent intermolecular interactions between protein and DNA. The *thicker arrow* between Leu-337 and one oxygen atom on +5′p represents the hydrogen bond that is augmented by the macrodipole of helix H1. The lines between structural modules have been replaced by *dashed lines* in the bound state to indicate the altered intramolecular interactions in the presence of DNA. The conformation change in inhibitory module is indicated by the altered symbol of the inhibitory module.

the helix H1, the hydrophobic interactions with the core of the ETS domain, and potentially polar and hydrophobic interactions with the inhibitory module. In the model of the unbound state, helix H1 packs with the rest of the ETS domain as well as with the inhibitory module, and helix HI-1 in this module is folded. Upon binding to DNA, the conformation change in the inhibitory module is caused by the DNA-induced repositioning of helix H1 and the ability of the interacting network surrounding helix H1 to undergo dynamic changes. Thus, the precise position of the N terminus of helix H1 serves as a regulatory point of Ets-1 DNA binding.

This model provides a clear direction for further structural studies. The structure and position of helix H1 in the bound state is known from several ETS domain-DNA complexes. The exact positioning and packing of helix H1 in the unbound state would define the connection to the structured inhibitory module. Furthermore, the comparison of helix H1-inhibitory module connections in the bound state *versus* the unbound state would establish the details of the proposed change in helix H1 that allosterically induces the unfolding of helix HI-1 upon DNA binding.

Biological Significance of Helix H1 as the Keystone of Autoinhibition—Autoinhibition is a common feature of the *ets* family of transcription factors. Our current structural and mechanistic model of Ets-1 autoinhibition provides new insight into how other *ets* family members could use this mechanism to modulate ETS domain DNA binding. Inhibitory sequences for DNA binding have been identified outside the ETS domains of ERM, Elk-1, SAP-1, NET, and PEA3 (37–43) as well as Ets-1 and Ets-2 (12, 44). However, except for Ets-1 and Ets-2, these Ets proteins share little sequence similarity outside of the ETS domain. On the other hand, sequences of helix H1 are highly conserved among all *ets* family members, and the helix H1-phosphate contact is observed in the high resolution structures of four different Ets proteins in complex with DNA (3–7). Therefore, the inhibitory sequences in other Ets proteins could form structural modules, albeit different from the one in Ets-1, and interact with helix H1 to regulate DNA binding.

Our model of Ets-1 autoinhibition suggests that a partner protein could regulate ETS domain DNA binding directly by interacting with helix H1 or indirectly through interactions

with inhibitory elements. Indeed, DNA binding cooperativity between Ets-1 and its protein partner CBFα2 (RUNX1) requires the inhibitory elements of Ets-1, suggesting that the partnership counteracts autoinhibition (35, 45). The Ets protein GABPα provides an alternative example. A crystallographic study of the GABPα/β complex (4) shows that GABPβ, although not binding DNA itself, interacts directly with the helix H1 of GABPα and enhances the DNA binding affinity. Interestingly, a glutamine in helix H1 of GABPα that interacts with the β subunit is analogous to glutamine 339 in Ets-1, which we proposed would contact the inhibitory elements. This glutamine is highly conserved in Ets proteins, including those that have inhibitory sequences. We speculate that this residue, which lies on a conserved surface of helix H1, can interact with either inhibitory elements or a partner protein and that this type of interaction might provide a common method for regulation of ETS domain DNA binding.

On a more global level, these observations provide new insight into the general phenomenon of allosteric regulation. The intermolecular and intramolecular networks of interactions that propagate the allosteric regulation of DNA binding in Ets-1 include a protein-DNA interaction. This contact is not in the core of the ETS domain-DNA interface, which displays direct contact between base pairs and amino acids, but rather in a region that displays only phosphodiester backbone interaction. We speculate that a phosphate-protein interaction, especially one networked to structural elements within the protein, would display the versatility suitable for playing a role in finely tuned regulation. In addition, this DNA contact is distinctive, being facilitated by the macrodipole of an α helix. We suggest that this type of bond, which could be responsive to the positioning of an entire helix, is a highly effective transmitter of allosteric signals.

REFERENCES

1. Sharrocks, A., Brown, A., Ling, Y., and Yates, P. (1997) *Int. J. Biochem. Cell Biol.* **29,** 1371–1387
2. Graves, B. J., and Petersen, J. M. (1998) in *Advances in Cancer Research* (Woude, G. V., and Klein, G., eds) Vol. 75, pp. 1–55, Academic Press, San Diego
3. Kodandapani, R., Pio, F., Ni, C.-Z., Piccialli, G., Klemsz, M., McKercher, S., Maki, R. A., and Ely, K. R. (1996) *Nature* **380,** 456–460
4. Batchelor, A., Piper, D., de la Brousse, F. C., Mcknight, S., and Wolberger, C. (1998) *Science* **279,** 1037–1041
5. Mo, Y., Vaessen, B., Johnston, K., and Marmorstein, R. (1998) *Mol. Cell* **2,** 201–212
6. Hassler, M., and Richmond, T. J. (2001) *EMBO J.* **20,** 3018–3028
7. Mo, Y., Vaessen, B., Johnston, K., and Marmorstein, R. (2000) *Nat. Struct. Biol.* **7,** 292–297
8. Crepieux, P., Coll, J., and Stehelin, D. (1994) *Crit. Rev. Oncog.* **5,** 615–638
9. Graves, B. J., Cowley, D. O., Goetz, T. L., Petersen, J. M., Jonsen, M. D., and Gillespie, M. E. (1998) *Cold Spring Harbor Symp. Quant. Biol.* **LXIII,** 621–629
10. Lim, F., Kraut, N., Frampton, J., and Graf, T. (1992) *EMBO J.* **11,** 643–652
11. Nye, J. A., Petersen, J. M., Gunther, C. V., Jonsen, M. D., and Graves, B. J. (1992) *Genes Dev.* **6,** 975–990
12. Hagman, J., and Grosschedl, R. (1992) *Proc. Natl. Acad. Sci. U. S. A.* **89,** 8889–8893
13. Jonsen, M. D., Petersen, J. M., Xu, Q. P., and Graves, B. J. (1996) *Mol. Cell. Biol.* **16,** 2065–2073
14. Skalicky, J. J., Donaldson, L. W., Petersen, J. M., Graves, B. J., and McIntosh, L. P. (1996) *Protein Sci.* **5,** 296–309
15. Petersen, J. M., Skalicky, J. J., Donaldson, L. W., McIntosh, L. P., Alber, T., and Graves, B. J. (1995) *Science* **269,** 1866–1869
16. Hol, W. G., van Duijnen, P. T., and Berendsen, H. J. (1978) *Nature* **273,** 443–446
17. Donaldson, L. W., Petersen, J. M., Graves, B. J., and McIntosh, L. P. (1996) *EMBO J.* **15,** 125–134
18. Gill, S. C., and von Hippel, P. H. (1989) *Anal. Biochem.* **182,** 319–326
19. Gunther, C. V., and Graves, B. J. (1994) *Mol. Cell. Biol.* **14,** 7569–7580
20. Pio, F., Kodandapani, R., Ni, C.-Z., Shepard, W., Klemsz, M., McKercher, S. R., Maki, R. A., and Ely, K. R. (1996) *J. Biol. Chem.* **271,** 23329–23337
21. Szymczyna, B. R., and Arrowsmith, C. H. (2000) *J. Biol. Chem.* **275,** 28363–28370
22. Mohibullah, N., Donner, A., Ippolito, J. A., and Williams, T. (1999) *Nucleic Acids Res.* **27,** 2760–2769
23. Aymami, J., Coll, M., van der Marel, G. A., van Boom, J. H., Wang, A. H., and Rich, A. (1990) *Proc. Natl. Acad. Sci. U. S. A.* **87,** 2526–2530
24. Snowden-Ifft, E. A., and Wemmer, D. E. (1990) *Biochemistry* **29,** 6017–6025
25. Lane, M. J., Paner, T., Kashin, I., Faldasz, B. D., Li, B., Gallo, F. J., and Benight, A. S. (1997) *Nucleic Acids Res.* **25,** 611–617
26. Pieters, J. M., Mans, R. M., van den Elst, H., van der Marel, G. A., van Boom, J. H., and Altona, C. (1989) *Nucleic Acids Res.* **17,** 4551–4565
27. Roll, C., Ketterle, C., Faibis, V., Fazakerley, G. V., and Boulard, Y. (1998) *Biochemistry* **37,** 4059–4070
28. Singh, S., Patel, P. K., and Hosur, R. V. (1997) *Biochemistry* **36,** 13214–13222
29. Garvie, C. W., and Phillips, S. E. (2000) *Structure* **8,** 905–914
30. Lesser, D. R., Kurpiewski, M. R., and Jen-Jacobson, L. (1990) *Science* **250,** 776–786
31. Wenz, C., Jeltsch, A., and Pingoud, A. (1996) *J. Biol. Chem.* **271,** 5565–5573
32. Harrison, S. C., and Aggarwal, A. K. (1990) *Annu. Rev. Biochem.* **59,** 933–969
33. Myszka, D. G., Jonsen, M. D., and Graves, B. J. (1998) *Anal. Biochem.* **265,** 326–330
34. Cowley, D. O., and Graves, B. J. (2000) *Genes Dev.* **14,** 366–376
35. Goetz, T. L., Gu, T. L., Speck, N. A., and Graves, B. J. (2000) *Mol. Cell. Biol.* **20,** 81–90
36. Jonsen, M. D. (1999) *Autoinhibition of DNA Binding in the Transcription Factor Ets-1: A Mechanistic and Structural Study.* Ph.D. thesis, University of Utah, Salt Lake City
37. Laget, M.-P., Defossez, P.-A., Albagli, O., Baert, J.-L., Dewitte, F., Stehelin, D., and de Launoit, Y. (1996) *Oncogene* **12,** 1325–1336
38. Price, M. A., Rogers, A. E., and Treisman, R. (1995) *EMBO J.* **14,** 2589–2601
39. Yang, S. H., Shore, P., Willingham, N., Lakey, J. H., and Sharrocks, A. D. (1999) *EMBO J.* **18,** 5666–5674
40. Dalton, S., and Treisman, R. (1992) *Cell* **68,** 597–612
41. Giovane, A., Pintzas, A., Maira, S., Sobieszczuk, P., and Wasylyk, B. (1994) *Genes Dev.* **8,** 1502–1513
42. Greenall, A., Willingham, N., Cheung, E., Boam, D. S., and Sharrocks, A. D. (2001) *J. Biol. Chem.* **17,** 17
43. Bojovic, B. B., and Hassell, J. A. (2001) *J. Biol. Chem.* **276,** 4509–4521
44. Cowley, D. O. (2000) *Ets-1 and Ets-2 Regulation.* Ph.D. thesis, University of Utah, Salt Lake City
45. Gu, T. L., Goetz, T. L., Graves, B. J., and Speck, N. A. (2000) *Mol. Cell. Biol.* **20,** 91–103
46. Werner, M. H., Clore, G. M., Fisher, C. L., Fisher, R. J., Trinh, L., Shiloach, J., and Gronenborn, A. M. (1997) *J. Biomol. NMR* **10,** 317–328
47. Gillespie, M. E. (1998) *A Structural and Genetic Investigation of Ets-1.* Ph.D. thesis, University of Utah, Salt Lake City
48. Brown, T. A., and McKnight, S. L. (1992) *Genes Dev.* **6,** 2502–2512
49. Ray-Gallet, D., Mao, C., Tavitian, A., and Moreau-Gachelin, F. (1995) *Oncogene* **11,** 303–313
50. Shore, P., and Sharrocks, A. D. (1995) *Nucleic Acids Res.* **23,** 4698–4706